Molecular Immunology 105 (2019) 9–15

Contents lists available at ScienceDirect

Molecular Immunology

journal homepage: www.elsevier.com/locate/molimm

Distribution of mast cells within the mouse heart and its dependency on *Mitf*

Arnar Bragi Ingason[a,b], Fatich Mechmet[b], Diahann Alexandra Maria Atacho[a,b], Eiríkur Steingrímsson[a], Pétur Henry Petersen[b,*]

[a] Department of Biochemistry and Molecular Biology, Biomedical Center, Faculty of Medicine, University of Iceland, Reykjavik, Iceland
[b] Department of Anatomy, Biomedical Center, Faculty of Medicine, University of Iceland, Reykjavik, Iceland

ARTICLE INFO

Keywords:
Mice
Mast cells
Microphthalmia-associated transcription factor
Heart
Chymase

ABSTRACT

Although mast cell distribution has been described in both human and canine hearts, cardiac mast cells in mice have yet to be categorically localized. We therefore sought to describe mast cell distribution within the mouse heart and characterize their dependence on the Microphthalmia-associated transcription factor (*Mitf*). Cardiac mast cells were visualized using Toluidine Blue and avidin staining, and their distribution within the heart described. Cardiac mast cells were most prevalent in the epicardium (50%) or myocardium (45%). Less frequently, mast cells were noted in the endocardium (5%). Within the myocardium, 31% of the mast cells had perivascular location. By studying two different *Mitf* mutant strains, $Mitf^{mi\text{-}vga9}$ and $Mitf^{Mi\text{-}wh}$, we demonstrated that these mutations led to near-complete deficiency of cardiac mast cells. Accordingly, expression of the *mMCP-4* and *mMCP-5* genes was lost and chymase enzyme activity was severely reduced. Additionally, hearts from mice heterozygous for these *Mitf* mutations contained significantly fewer mast cells compared to wild-type mice. Our results demonstrated that the distribution of cardiac mast cells in mice is different from humans and dogs. Cardiac mast cells are dependent on *Mitf* expression, with loss-of-function mutation in the *Mitf* gene leading to near-complete lack of cardiac mast cells. Loss of a single *Mitf* allele is sufficient for relative mast cell deficiency.

1. Introduction

Mast cells are primarily known for their role in allergic and anaphylactic reactions. However, studies have demonstrated that mast cells have various other physiological and pathological effects in peripheral tissues, including the heart (da Silva et al., 2014). Mast cells play an important role in heart pathology and have been linked to various cardiovascular diseases such as atherosclerosis, myocardial ischemia, heart failure, and cardiac hypertrophy (Alevizos et al., 2014; Bot et al., 2015; Hara et al., 2002; Reid et al., 2007). Importantly, the role of mast cells differs depending on their location. This stems from the fact that mast cell progenitors migrate to peripheral tissues, through organ-specific migration pathways and it is the microenvironment of these organs which stimulates mast cell differentiation (Gurish and Austen, 2012). In accordance with this, cardiac mast cells have been shown to differ functionally from other organ-specific mast cells (Patella et al., 1995). Whereas the distribution of cardiac mast cells has been described in humans and dogs (Frangogiannis et al., 1999; Hellstrom and Holmgren, 1950; Sperr et al., 1994), their distribution in mice is not well characterized. This is unfortunate, as the mouse is the most widely used genetic model of cardiac physiology and pathology.

Here, we describe the distribution of mast cells within the mouse heart and compare it with mast cell distribution in other mammalian species. The Microphthalmia-associated transcription factor (MITF) is a basic helix-loop-helix leucine zipper master regulator that plays a critical role in the development of many cell types, including mast cells (Hemesath et al., 1994; Steingrimsson et al., 2004). We examined whether hearts from mice carrying two different *Mitf* mutations ($Mitf^{mi\text{-}vga9}$ and $Mitf^{Mi\text{-}wh}$) are mast cell deficient, and whether this is gene dosage dependent.

2. Methods

2.1. Animal handling

C57BL/6 J, C57BL/6-$Mitf^{mi\text{-}vga9}$ and C57BL/6-$Mitf^{Mi\text{-}wh}$ mice were housed and bred in the animal facility at the University of Iceland. The use of laboratory animals was approved by the Icelandic Food and Veterinary Authority (permit ID: 2013-03-01). Maintenance and handling of animals was performed in accordance with Icelandic and European legislation on animal welfare.

* Corresponding author at: Department of Anatomy, Biomedical Center, Faculty of Medicine, University of Iceland, Vatnsmýrarvegur 16, 101, Reykjavik, Iceland.
E-mail address: phenry@hi.is (P.H. Petersen).

https://doi.org/10.1016/j.molimm.2018.11.009
Received 30 April 2018; Received in revised form 16 October 2018; Accepted 14 November 2018
Available online 22 November 2018

2.2. Histological staining and analysis

Mice were sacrificed and hearts fixed in formalin. Subsequently, the hearts were embedded in paraffin and 4 µm thick sagittal sections obtained, mounted, and stained with Toluidine Blue and avidin to visualize cardiac mast cells.

For avidin staining, the tissue sections were deparaffinized by xylene and then rehydrated with ethanol twice for 5 minutes each. Next, the slides were incubated in citrate buffer (p = 6.0) for 20 min at 95° for antigen retrieval. After cooling, slides were treated with 10% fetal bovine serum for 1 h at room temperature (RT). Subsequently, sections were rinsed with immunofluoroscence (IF) buffer containing 0.15 M NaCl, 5 mM EDTA, 20 mM HEPES, and 0.1% Triton X-100 (pH = 7.5). Sections were then stained with Alexa Fluor 488 conjugated avidin at the dilution of 1:500 (Invitrogen, Austin, TX) and counterstained with 4′,6-diamidino-2-phenylindole (DAPI) 1:5000 (Sigma, St. Louis, MO) diluted in IF buffer for 1 h at RT. Lastly, sections were rinsed twice with IF buffer for 5 min, once with distilled water, and coverslip added following dehydration.

For mast cell quantification, Toluidine Blue positive cells and avidin positive cells were counted in two whole sections from each heart. Using the Fiji software, area measurements were performed, and mast cells quantified as cells per mm^2 within different regions of the heart.

2.3. Enzyme activity assays

Mice were sacrificed and hearts snap frozen in liquid nitrogen. Frozen hearts were put in 1 mL of TrisHCl buffer containing 0.5 M NaCl and 1 mM EDTA (pH = 8.0) buffer along with 20 µL of aprotinin and pulverized at 2600 rpm for 30 s. Sonication was thereafter performed for 5 min, followed by centrifugation at 14,000 rpm for 10 min. The supernatant was collected for analysis. Bradford assay was performed to estimate protein amount and heart samples diluted in TrisHCl buffer, containing 0.5 M NaCl and 1 mM EDTA (pH = 8.0), to 2200 µg/mL (Bradford, 1976).

For chymase activity assay, a solution containing 29.7 µL of 11 mM Suc-AAPF (Sigma-Aldrich, St. Louis, MO) and 240 µL of TrisHCl buffer containing 0.5 M NaCl and 1 mM EDTA (pH = 8.0) was prepared for each sample and allowed to incubate for 10 min. Thereafter, 60 µL of sample was added and allowed to incubate for 10 min, before adding 20 µL of 10 mM chymostatin (Sigma-Aldrich) to stop the reaction. Lastly, solutions were transferred to a 96 well plate (using 90 µL triplicates from each sample) and absorbance measured at 405 nm using EMax Plus Microplate Reader (Molecular Devices, Sunnyvale, CA).

Phosphatase activity assay was performed according to manufacturer's suggestions with some modifications (Sigma-Aldrich). Briefly, for each sample, 10 µL of 0.67 nM pNPP solution were added to 0.58 mL of diethanolamine buffer containing 0.50 mM magnesium chloride (pH = 9.8), and allowed to incubate at 37° for 10 min. Thereafter, 10 µL of sample was added and allowed to incubate for 10 min before the reaction was stopped by adding 3 M NaOH. Lastly, solutions were transferred to a 96 well plate (using 150 µL triplicates for each sample) and absorbance measured at 405 nm using EMax Plus Microplate Reader (Molecular Devices, Sunnyvale, CA).

2.4. Quantitative real-time PCR

For quantitative real-time PCR, mice were sacrificed and hearts snap frozen in liquid nitrogen. Hearts were pulverized twice at 2600 rpm for 30 s and RNA isolated according to protocol (Chomczynski and Sacchi, 1987). Next, cDNA was generated using Superscript II (Invitrogen) and oligo(d)T primer mix. Real time PCR was performed using Power SYBR Green PCR Master Mix (ThermoFisher Scientific, Waltham, MA). The following primers were used for amplification: *Actin* sense, 5'-CAC TGT CGA GTC GCG TCC-3'; *Actin* antisense, 5'-TCA TCC ATG GCG AAC TGG TG-3'; *Mitf* sense, 5'-AGC AAG AGC ATT GGC TAA AGA-3'; *Mitf* antisense, 3'-GCA TGT CTG GAT CAT TTG ACT-'5'; *mMCP-4* sense, 5'-GCC AAA GAG ACT CCC TCT GTG ATT-3'; *mMCP-4* antisense, 3'-GCA TCT CCG CGT CCA TAA GAT ACA-'5'; *mMCP-5* sense, 5'-CAC TGT GCG GGA AGG TCT ATA ACA-3'; *mMCP-5* antisense, 3'-TT ACT TCC TGC AGT GTG TCG GAG-'5'.

2.5. Statistical analysis

All data are presented as mean ± SEM unless otherwise specified. The Wilcoxon test was used to compare differences between two groups. The Kruskal Wallis test was used to compare differences between multiple groups. The Conover test with Bonferroni correction was used as a post hoc test. All statistical tests were two-tailed and a P value less than 0.05 was considered significant.

3. Results

3.1. Distribution and localization of cardiac mast cells

To describe the location of mast cells within the heart, sagittal sections from wild-type (C57BL/6 J) mouse hearts were obtained and stained with Toluidine Blue in order to visualize mast cells. Mast cells were quantified in the epicardium, myocardium, and endocardium of the left and right ventricles and atria. Mast cells found within the heart valves, aorta, pulmonary vessels, and the fibrous and parietal pericardium were excluded from quantification since these were not consistently present in the samples. The majority of mast cells were located in the epicardium (Fig. 1a, e) or within the interstitium of the myocardium (Fig. 1b, f). They were less frequently observed in the endocardium (Fig. 1c, g) or within the adventitia of myocardial arterioles or venules (Fig. 1d, h). Within the myocardium, 31% of the mast cells had perivascular location (Table 1).

When adjusted for area, mast cell density was more than twelvefold higher in the epicardium than in the myocardium or endocardium,

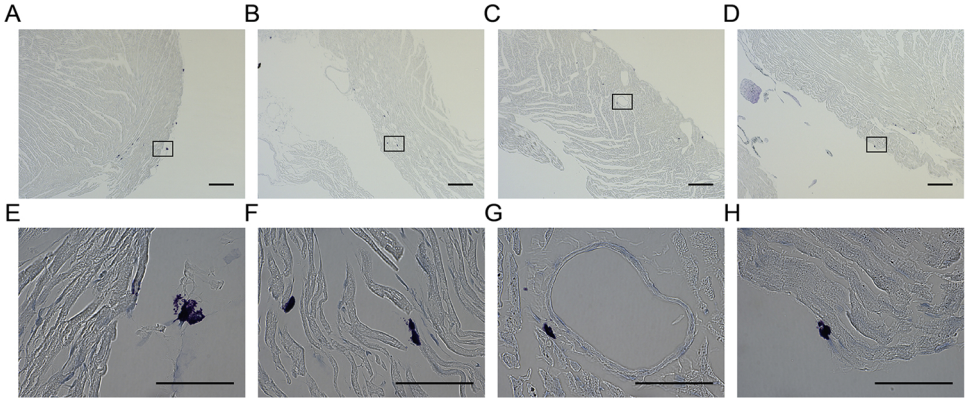

Fig. 1. Distribution of mast cells within the mouse heart. Mast cells visualized by Toluidine Blue staining were most prevalent in a) the epicardium and b) within the interstitium of the myocardium. Mast cells were less frequently found within c) the endocardium or d) within the adventitia of myocardial arteries or veins. e–h) High magnification images of the boxed areas in a–d) are provided below. Scale bars represent 200 µm in a–d) and 20 µm in e–h) (For interpretation of the references to colour in this figure legend, the reader is referred to the web version of this article).

Table 1
Mast Cell Distribution in Wild-Type and Heterozygous Mitf Mutant Hearts.

Location	Proportion of total mast cells (%)[a]		
	WT (n = 21)	*Mitf*$^{Mi\text{-}wh}$/+ (n = 5)	*Mitf*$^{mi\text{-}vga9}$/+ (n = 17)
Epicardium	50 ± 2	55 ± 5	56 ± 4
Myocardium	45 ± 2	43 ± 5	40 ± 4
Interstitial	69 ± 4	80 ± 7	75 ± 4
Perivascular	31 ± 4	20 ± 7	25 ± 4
Endocardium	5 ± 1	3 ± 2	4 ± 1
Atria	8 ± 2	11 ± 5	8 ± 3
Left ventricle	54 ± 3	59 ± 4	54 ± 4
Right ventricle	24 ± 2	31 ± 4	29 ± 2
Septum	14 ± 2	3 + 2*	9 ± 3

Asterisks denote statistical significance at P < 0.05 (*) compared to wild-type mice.

[a] The mast cell proportion is calculated as the number of mast cells in a particular region divided by the total number of mast cells in the heart.

Table 2
Mast Cells Density in Wild-Type Hearts.

Location	WT (n = 21)
Epicardium	8.29 ± 0.59
Myocardium	0.56 ± 0.05
Endocardium	0.64 ± 0.09
Atria	2.40 ± 0.46
Left ventricle	1.09 ± 0.09
Right ventricle	2.10 ± 0.25
Septum	0.52 ± 0.10

Mast cell density is given as mast cells per mm^2.

which had similar mast cell densities (8.29 ± 0.59 cells/mm^2 vs 0.56 ± 0.05 cells/mm^2 and 0.64 ± 0.09 cells/mm^2 respectively) (Table 2). When looking at the different chambers of the heart, mast cell density was significantly higher in the atria as compared to the ventricles (2.40 ± 0.46 cells/mm^2 vs 1.03 ± 0.06 cells/mm^2, p = 0.03). Furthermore, mast cell density was lowest in the septum (0.52 ± 0.10 cells/mm^2), and significantly higher in the right ventricle as compared to the left ventricle (2.10 ± 0.25 cells/mm^2 vs 1.09 ± 0.09 cells/ mm^2, p < 0.001) (Table 2).

To confirm our findings, histological staining was performed using avidin, a marker that has been demonstrated to bind mast cell granules specifically (Tharp et al., 1985). Consistently, quantification of avidin positive cells demonstrated similar mast cell distribution as described above (Suppl. Table 1).

3.2. Mitf mutation leads to cardiac mast cell deficiency

Microphthalmia-associated Transcription Factor (MITF) is a basic helix-loop-helix leucine zipper master regulator that plays a critical role in mast cell differentiation (Qi et al., 2013). To assess the effects of *Mitf* mutation on mast cell numbers in the heart we studied cardiac mast cells in two different *Mitf* mutant alleles, *Mitf*$^{mi\text{-}vga9}$ and *Mitf*$^{Mi\text{-}wh}$. Sagittal sections from hearts of wild-type (C57BL/6 J) mice as well as hetero- and homozyogous *B6-Mitf*$^{Mi\text{-}wh}$ and *B6-Mitf*$^{mi\text{-}vga9}$ mutant mice were examined. The *Mitf*$^{mi\text{-}vga9}$ mutant allele contains a transgene insertion resulting in severely reduced expression of the Mitf mRNA (Hodgkinson et al., 1993; Kataoka et al., 2002). The *Mitf*$^{Mi\text{-}wh}$ mutant allele contains a point mutation that affects DNA binding but has little effect on Mitf expression (Kataoka et al., 2002; Steingrimsson et al., 1994). Homozygotes carrying the *Mitf*$^{mi\text{-}vga9}$ mutation are characterized by the absence of mast cells in the peritoneum, mesentery, and stomach. Additionally, mast cell numbers in the skin are reduced to one third of the number observed in the skin of wild type mice (Kataoka et al., 2002; Morii et al., 2004a). Mast cells are absent from the peritoneum of *Mitf*$^{Mi\text{-}wh}$/*Mitf*$^{Mi\text{-}wh}$ mice whereas their numbers are normal in the mesentery and skin (Jippo et al., 2003; Kim et al., 1999; Morii et al., 2004a). Cardiac mast cells were near absent from *Mitf*$^{mi\text{-}vga9}$ and *Mitf*$^{Mi\text{-}wh}$ homozygous mice and significantly fewer than in both heterozygotes for each mutation and wild-type (Fig. 2a,c). Mice homozygous for the *Mitf*$^{Mi\text{-}wh}$ mutation trended towards higher mast cell numbers than *Mitf*$^{mi\text{-}vga9}$ homozygous mice (0.09 ± 0.03 mast cells/mm^2 vs 0.001 ± 0.001 mast cells/mm^2, p = 0.10). Interestingly, the number of mast cells found in *Mitf*$^{mi\text{-}vga9}$/+ heterozygous hearts was reduced by half as compared to wild-type hearts (0.54 ± 0.07 mast cells/mm^2 vs 1.06 ± 0.06 mast cells/mm^2, p < 0.001) (Fig. 3a). *Mitf*$^{Mi\text{-}wh}$/+ heterozygotes had approximately two thirds of the number of mast cells found in wild type hearts (0.71 ± 0.07 mast cells/mm^2 vs 1.06 ± 0.06 mast cells/mm^2, p = 0.04). To confirm the reduction in mast cell numbers in Mitf mutants, we performed avidin staining on *Mitf*$^{mi\text{-}vga9}$ hetero- and homozygotes. Consistently, avidin staining demonstrated near absence of cardiac mast cells in *Mitf*$^{mi\text{-}vga9}$ homozygotes (0.01 ± 0.01 mast cells/mm^2), and relative reduction in mast cell numbers in *Mitf*$^{mi\text{-}vga9}$ heterozygotes compared to wild-type hearts (0.52 ± 0.08 mast cells/mm^2 vs 1.08 ± 0.35 mast cells/mm^2, p = 0.04) (Fig. 2b, d). Taken together, this demonstrates that Mitf is necessary for normal cardiac mast cell numbers and that a single mutant allele is sufficient for relative mast cell deficiency.

To estimate whether the reduced numbers of cardiac mast cells in heterozygotes affected the distribution of mast cells within the heart, we compared the mast cell distribution within different regions of the heart between wild-type, *Mitf*$^{mi\text{-}vga9}$/+, and *Mitf*$^{Mi\text{-}wh}$/+ heterozygotes. The mast cell distribution was generally similar in the three genotypes. However, the percentage of mast cells within the septum of *Mitf* $^{Mi\text{-}wh}$/ + heterozygotes was significantly reduced compared to wild-type mice (p = 0.03) (Table 1).

3.3. Chymase activity and expression is absent from Mitf mutant hearts

Chymase is a mast cell-specific serine protease that is commonly used as a mast cell marker (Craig and Schwartz, 1989). Humans have a single chymase gene, whereas mice have five. Real-time PCR was performed to determine the expression of *mMCP-4* and *mMCP-5*, the two mouse chymases that are functionally and structurally closest to the human chymase, respectively (Pejler et al., 2010). Our results demonstrated severely reduced expression of both *mMCP-4 and mMCP-5* in homozygous *Mitf*$^{mi\text{-}vga9}$ hearts compared to wild-type hearts (p < 0.001 for both genes) (Fig. 3a,b). Additionally, *mMCP-5* expression in heterozygous *Mitf*$^{mi\text{-}vga9}$ hearts was significantly lower than in wild-type hearts (p = 0.015). Similarly, *mMCP-4* trended towards lower expression in heterozygotes compared to wild-type hearts (p = 0.11). Consistent with the effects of the *Mitf*$^{mi\text{-}vga9}$ mutation, expression of *Mitf* in the heart was absent from homozygotes and reduced to approximately 40% in heterozygotes as compared to wild type mice (Fig. 3c).

Chymase enzymatic activity was determined to evaluate whether reduced chymase expression led to reduced functional activity of the enzyme. Our results demonstrated that chymase activity was severely reduced in *Mitf*$^{mi\text{-}vga9}$/*Mitf*$^{mi\text{-}vga9}$ hearts (Fig. 3d). Although chymase activity was also reduced in heterozygotes, the difference was not statistically significant. Alkaline phosphatase activity was used as a control measurement and no differences were observed between the three groups (Fig. 3e). We conclude that there is a near-complete loss of mature mast cells and mast-cell specific chymase in *Mitf*$^{mi\text{-}vga9}$ mutant mice.

4. Discussion

Mast cells have been linked to various cardiovascular diseases (Reid et al., 2007). Here we demonstrate that mast cells distribution is

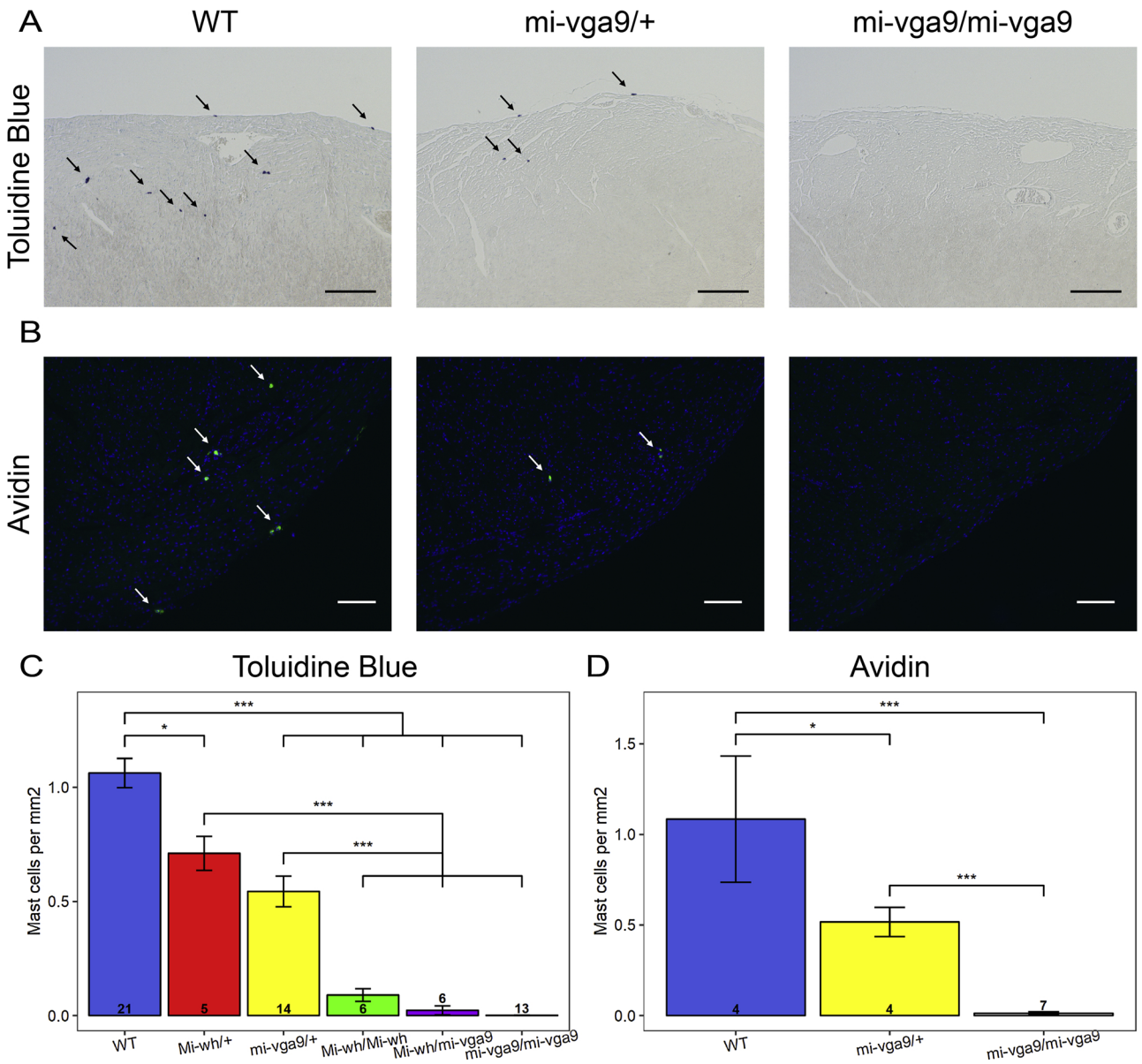

Fig. 2. Mif mutation leads to cardiac mast cell deficiency. A–B) Cardiac mast cells were identified using Toluidine Blue and avidin staining. The number of Toluidine Blue and avidin positive cells are compared between wild-type mice and mice hetero- or homozygous for the *Mitf*$^{mi\text{-}vga9}$ mutations. Arrows point to mast cells. Scale bars represent 200 μm. For A) purple = Toluidine Blue. For B) green = avidin, blue = DAPI. C–D) Bar graphs comparing cardiac mast cell density in wild-type mice and mice hetero- and homozygous for the *Mitf* $^{mi\text{-}vga9}$ and *Mitf*$^{Mi\text{-}wh}$ mutations, using Toluidine Blue staining and avidin staining respectively. Both graphs demonstrate near-complete lack of cardiac mast cells in homozygous *Mitf* mutant hearts, and significant reduction of mast cell numbers in heterozygotes compared to wild-type mice. Asterisks denote statistical significance at $P < 0.05$ (*), and $P < 0.001$ (***) (For interpretation of the references to colour in this figure legend, the reader is referred to the web version of this article).

different in mouse hearts, compared to humans. This is important as the mouse remains the most widely used genetic model of human physiology and pathology. Although the distribution of cardiac mast cells has been described in humans and dogs (Frangogiannis et al., 1999; Hellstrom and Holmgren, 1950; Sperr et al., 1994), this is to our best knowledge the first time that mast cell distribution has been categorically described in mouse hearts. Cardiac mast cells in mice are most prominent within the epicardium (50%) and the myocardium (45%). They are less frequently found within the endocardium (5%). When adjusted for area, mast cell density is highest in the epicardium, whereas it is lower but similar in the myocardium and the endocardium. The high density of epicardial mast cells is interesting since it has not been described in other mammalian species. Although epicardial mast cells in rats trend towards higher numbers compared to the endocardium (Facoetti et al., 2006), the difference in mice is twelvefold. Epicardial mast cells have also been described in humans but they have not been quantified (Sperr et al., 1994). The mouse myocardium and endocardium have approximately equal mast cell densities, similar to human and canine hearts (Frangogiannis et al., 1999; Sperr et al., 1994). Mast cell density in mice was found to be significantly higher in atrial appendages compared to ventricles. This is similar to humans but differs from dogs which have equal atrial and ventricular densities (Frangogiannis et al., 1999; Sperr et al., 1994). Taken together, this suggests that mast cell distribution is different between mammalian species.

When looking at the different chambers of the heart, mast cell density was greatest in the atria, followed by the right ventricle, left ventricle, and interventricular septum in descending order. Since the bulk of cardiac mast cells are located epicardially, this order is likely due to higher proportion of epicardium within these regions of the

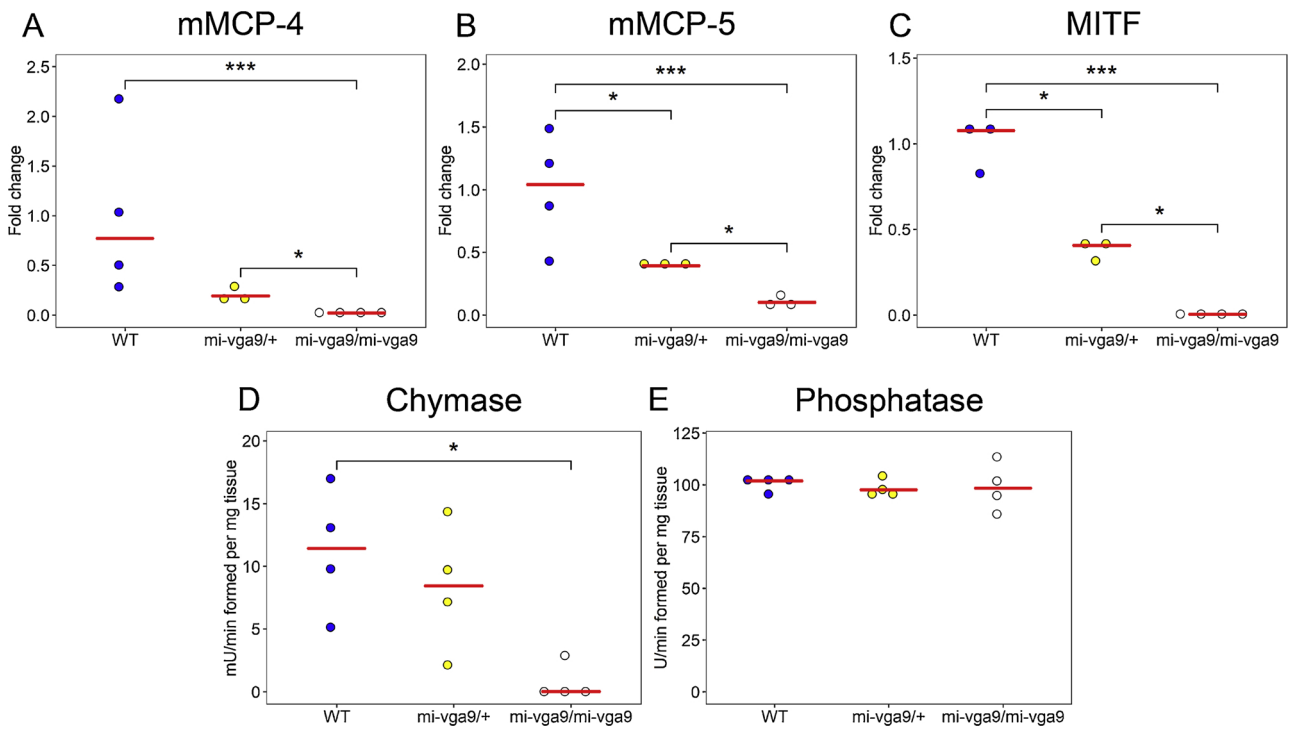

Fig. 3. Chymase activity and expression is absent from Mitf mutant hearts. a–c) Expression of mMCP4, mMCP5 and MITF in wild-type (WT), and hetero- and homozygous *Mitf*$^{mi\text{-}vga9}$ mutant hearts. Expression of all genes was significantly reduced in homozygous *Mitf*$^{mi\text{-}vga9}$ mutant hearts compared to wild-type and heterozygous *Mitf*$^{mi\text{-}vga9}$/+ hearts. d–e) Chymase and phosphatase activity assays in wild-type, hetero- and homozygous *Mitf*$^{mi\text{-}vga9}$ mutant hearts. Chymase activity was significantly reduced in homozygous *Mitf*$^{mi\text{-}vga9}$ mutant hearts compared to wild-type hearts. Phosphatase activity was similar between all genotypes. Red bars represent median value for each genotype. Asterisks denote statistical significance at $P < 0.05$ (*), and $P < 0.001$ (***) (For interpretation of the references to colour in this figure legend, the reader is referred to the web version of this article).

heart. Supporting this, the septum, which has no overlying epicardium, has similar mast cell density as both the myocardium and endocardium. In the current study, perivascular mast cells were defined as those found within the adventitia of myocardial arterioles or venules. We found that 31% of mouse mast cells residing in the myocardium have periarteriolar or perivenular location. For comparison, while 49% of canine cardiac mast cells have been described as perivascular, 27% had periarteriolar or perivenular location, which is consistent with our results.

In order to establish the role of cardiac mast cells in heart pathology it is important to establish diverse models of cardiac mast cell deficiency. Currently, only Kit-mutant and Cre/loxP-based mouse models are available (Feyerabend et al., 2011; Kitamura et al., 1978). Although *Mitf* mutant mice have been shown to have reduced numbers of mast cells in both the peritoneum and the skin (Jippo et al., 2003; Kataoka et al., 2002), the effect of *Mitf* in cardiac mast cells has not been documented previously. Here we report that cardiac mast cells are *Mitf* dependent and suggest that *Mitf* mutant mice may be a suitable model for investigating mast cell function in the heart. In the current study, mast cell deficiency in *Mitf* mutant hearts was demonstrated by Toluidine Blue and avidin staining, and by loss of mast cell-specific chymase activity and expression. This demonstrates that *Mitf*$^{mi\text{-}vga9}$ and *Mitf*$^{Mi\text{-}wh}$ homozygotes are cardiac mast cell depleted. Additionally, hearts from *Mitf*$^{mi\text{-}vga9}$/+ heterozygotes contained half the number of mast cells found in wild-type hearts. Interestingly, *Mitf*$^{Mi\text{-}wh}$/+ hearts trended towards mast cell numbers closer to wild type hearts. Similarly, *Mitf*$^{Mi\text{-}wh}$/*Mitf*$^{Mi\text{-}wh}$ and *Mitf*$^{Mi\text{-}wh}$/*Mitf*$^{mi\text{-}vga9}$ mice, while both severely cardiac mast cell deficient trended towards higher mast cell numbers than *Mitf*$^{mi\text{-}vga9}$ homozygotes. The *Mitf*$^{mi\text{-}vga9}$ mutation leads to the absence of *Mitf* expression (Hodgkinson et al., 1993), whereas the *Mitf*$^{Mi\text{-}wh}$ mutation is less severe, with retained *Mitf* expression and reduced but measurable DNA binding ability and nuclear localization (Kataoka et al., 2002; Kim et al., 1999; Morii et al., 1994). This difference may explain the higher mast cell numbers in the latter. Indeed, this has been demonstrated in other tissues, such as the skin, where *Mitf*$^{Mi\text{-}wh}$/*Mitf*$^{Mi\text{-}wh}$ mice have normal mast cell numbers as opposed to *Mitf*$^{mi\text{-}vga9}$/*Mitf*$^{mi\text{-}vga9}$ mice which have reduced numbers (Kataoka et al., 2002).

In addition to guiding mast cell differentiation, MITF regulates the expression of many mast cell-specific genes, including chymases. Chymase is an angiotensin II-forming serine protease that is secreted from mast cells following acute or chronic stimuli. In the *Mitf*$^{mi\text{-}vga9}$ mutant heart both chymase expression and enzymatic activity is lost, as expected. Additionally, hearts from *Mitf*$^{mi\text{-}vga9}$/+ heterozygotes have both reduced numbers of cardiac mast cells and reduced chymase expression compared to wild-type hearts. This suggests that both alleles of *Mitf* are required for normal cardiac mast cell numbers. Since *Mitf* plays a key role in mast cell development, the loss of cardiac mast cells in *Mitf* mutants is likely due to failure of mast cell differentiation. Alternatively, it may be explained by defective migration. As mast cell precursor cells migrate from the bone marrow and differentiate in their target environment, it is possible that the local environment affects cardiac mast cell localization. Supporting this, *Mitf* is not only expressed in mast cells in the heart, but also cardiomyocytes and valvular melanocytes (Tshori et al., 2007; Yajima and Larue, 2008). A study examining the role of *Mitf* in mast cell development demonstrated that bone marrow transplantation from a wild-type host to an *Mitf*$^{mi\text{-}vga9}$ homozygote recipient led to reduced mast cell density in skin, peritoneum, mesentery, stomach, and spleen. Interestingly, transplantation of *Mitf*$^{mi\text{-}vga9}$ homozygous bone marrow cells to W/W^{v} mice, a strain with mast cell deficiency but normal tissue environment, also led to reduced mast cell density (Morii et al., 2004b). Consistently, the cardiac mast cell deficiency observed in our study may be due to combination of both defective intracellular pathways in mast cell precursor cells and changes in the local environment.

The loss of cardiac mast cells and chymase activity has major implications for heart pathology. Chymase, angiotensin I converting enzyme (ACE), and cathepsin G all degrade Angiotensin I (Ang I) to

Angiotensin II (Ang II). In the blood, circulating serine protease inhibitors restrict chymase and cathepsin G activity (Tojo and Urata, 2013). Ang II formation is therefore mostly contributed by ACE activity in the blood, while chymase seems to be the principal Ang II forming enzyme in the heart (Urata et al., 1993). Mast cell derived-chymase has been linked to a role in various cardiovascular diseases, such as atherosclerosis, arrhythmias, heart failure, and hypertrophy (Reid et al., 2007). As well as being the key Ang II-forming enzyme in the heart, chymase directly induces activation of TGF-β (Lindstedt et al., 2001). TGF-β has been shown to be a downstream mediator of Ang II-induced cardiac hypertrophy (Schultz et al., 2002). Furthermore, chymase induces extracellular matrix degradation, cardiomyocyte apoptosis, and fibroblast proliferation (Hara et al., 1999; Janicki et al., 2006). These are all key characteristics in hypertrophy of failing hearts. Cardiac hypertrophy occurs in response to increased cardiac load. Interestingly, *Mitf* is required for cardiac hypertrophy in response to β-adrenergic or Ang II stimulation in mice, and *Mitf* mutant hearts fail to appropriately respond to these hypertrophic stimuli (Liu et al., 2014; Tshori et al., 2006). There is added complexity due to the fact that in the heart *Mitf* is not only expressed in mast cells but in cardiomyocytes as well. In fact, *Mitf* has been shown to induce cardiac hypertrophy through negatively regulating mi-R541 expression in cardiomyocytes (Liu et al., 2014). This hypertrophic response was induced by Ang II treatment, which, as stated above, is primarily generated by chymase (Urata et al., 1993). Based on the complete loss of chymase activity in the $Mitf^{mi\text{-}vga9}$ mutant heart we suggest that the role of *Mitf* in inducing cardiac hypertrophy is, at least in part, mast cell and chymase dependent.

Our results must be interpreted in the context of several limitations. First, as mast cells differentiate in their target environment, we cannot exclude the possibility that cardiac mast cell progenitor cells, that do not contain granules or express the major mast cell proteases, may be present in *Mitf* mutant mice. If so, they are unlikely to be functional as mast cells. Second, all quantification and distribution measurements were acquired using sagittal sections. It is possible that mast cell localization differs in lateral sections. Whole mount staining may be performed for better visualization of mast cells within the whole heart. Lastly, our distribution analysis was gathered by studying C57BL/6 J mice, the most commonly used inbred mouse strain. Further analysis of different mouse strains is needed to determine whether the distribution observed is specific to the C57BL/6 J strain.

5. Conclusions

Our results demonstrate that the distribution of cardiac mast cells in mice is different from humans and dogs. This is particularly important since mice remain the most widely used animal model for cardiac pathology and physiology. The different cellular composition of mammalian hearts must be considered when basic research from animal models is translated to clinical settings. In addition, we demonstrate that cardiac mast cells are *Mitf* dependent, with loss-of-function mutation in the *Mitf* gene leading to near-complete lack of mature cardiac mast cells.

Disclosures

The authors report no conflicts of interest.

Source of funding

This research was supported by grants from the Icelandic Research Fund [grant numbers: 152715-053 and 163068-051]. The funding source had no involvement in the study design, data collection or analysis, the submission process, or any other aspect of the research conduction.

Appendix A. Supplementary data

Supplementary material related to this article can be found, in the online version, at doi:https://doi.org/10.1016/j.molimm.2018.11.009.

References

Alevizos, M., et al., 2014. Stress triggers coronary mast cells leading to cardiac events. Ann. Allergy Asthma Immunol. 112, 309–316.
Bot, I., et al., 2015. Mast cells as effectors in atherosclerosis. Arterioscler. Thromb. Vasc. Biol. 35, 265–271.
Bradford, M.M., 1976. A rapid and sensitive method for the quantitation of microgram quantities of protein utilizing the principle of protein-dye binding. Anal. Biochem. 72, 248–254.
Chomczynski, P., Sacchi, N., 1987. Single-step method of RNA isolation by acid guanidinium thiocyanate-phenol-chloroform extraction. Anal. Biochem. 162, 156–159.
Craig, S.S., Schwartz, L.B., 1989. Tryptase and chymase, markers of distinct types of human mast cells. Immunol. Res. 8, 130–148.
da Silva, E.Z., et al., 2014. Mast cell function: a new vision of an old cell. J. Histochem. Cytochem. 62, 698–738.
Facoetti, A., et al., 2006. Histochemical study of cardiac mast cells degranulation and collagen deposition: interaction with the cathecolaminergic system in the rat. Eur. J. Histochem. 50, 133–140.
Feyerabend, T.B., et al., 2011. Cre-mediated cell ablation contests mast cell contribution in models of antibody- and T cell-mediated autoimmunity. Immunity 35, 832–844.
Frangogiannis, N.G., et al., 1999. Histochemical and morphological characteristics of canine cardiac mast cells. Histochem. J. 31, 221–229.
Gurish, M.F., Austen, K.F., 2012. Developmental origin and functional specialization of mast cell subsets. Immunity 37, 25–33.
Hara, M., et al., 1999. Mast cells cause apoptosis of cardiomyocytes and proliferation of other intramyocardial cells in vitro. Circulation 100, 1443–1449.
Hara, M., et al., 2002. Evidence for a role of mast cells in the evolution to congestive heart failure. J. Exp. Med. 195, 375–381.
Hellstrom, B., Holmgren, H., 1950. Numerical distribution of mast cells in the human skin and heart. Acta Anat. (Basel) 10, 81–107.
Hemesath, T.J., et al., 1994. microphthalmia, a critical factor in melanocyte development, defines a discrete transcription factor family. Genes Dev. 8, 2770–2780.
Hodgkinson, C.A., et al., 1993. Mutations at the mouse microphthalmia locus are associated with defects in a gene encoding a novel basic-helix-loop-helix-zipper protein. Cell 74, 395–404.
Janicki, J.S., et al., 2006. Cardiac mast cell regulation of matrix metalloproteinase-related ventricular remodeling in chronic pressure or volume overload. Cardiovasc. Res. 69, 657–665.
Jippo, T., et al., 2003. Effect of anatomical distribution of mast cells on their defense function against bacterial infections: demonstration using partially mast cell-deficient tg/tg mice. J. Exp. Med. 197, 1417–1425.
Kataoka, T.R., et al., 2002. Dual abnormal effects of mutant MITF encoded by Mi(wh) allele on mouse mast cells: decreased but recognizable transactivation and inhibition of transactivation. Biochem. Biophys. Res. Commun. 297, 111–115.
Kim, D.K., et al., 1999. Different effect of various mutant MITF encoded by mi, Mior, or Miwh allele on phenotype of murine mast cells. Blood 93, 4179–4186.
Kitamura, Y., et al., 1978. Decrease of mast cells in W/Wv mice and their increase by bone marrow transplantation. Blood 52, 447–452.
Lindstedt, K.A., et al., 2001. Activation of paracrine TGF-β1 signaling upon stimulation and degranulation of rat serosal mast cells: a novel function for chymase. Faseb J. 15, 1377–1388.
Liu, F., et al., 2014. Cardiac hypertrophy is negatively regulated by miR-541. Cell Death Dis. 5, e1171.
Morii, E., et al., 2004a. Number of mast cells in the peritoneal cavity of mice: influence of microphthalmia transcription factor through transcription of newly found mast cell adhesion molecule, spermatogenic immunoglobulin superfamily. Am. J. Pathol. 165, 491–499.
Morii, E., et al., 2004b. Roles of MITF for development of mast cells in mice: effects on both precursors and tissue environments. Blood 104, 1656–1661.
Morii, E., et al., 1994. Loss of DNA binding ability of the transcription factor encoded by the mutant mi locus. Biochem. Biophys. Res. Commun. 205, 1299–1304.
Patella, V., et al., 1995. Human heart mast cells: a definitive case of mast cell heterogeneity. Int. Arch. Allergy Immunol. 106, 386–393.
Pejler, G., et al., 2010. Mast cell proteases: multifaceted regulators of inflammatory disease. Blood 115, 4981–4990.
Qi, X., et al., 2013. Antagonistic regulation by the transcription factors C/EBPalpha and MITF specifies basophil and mast cell fates. Immunity 39, 97–110.
Reid, A.C., et al., 2007. Renin: at the heart of the mast cell. Immunol. Rev. 217, 123–140.
Schultz, J.E.J., et al., 2002. TGF-β1 mediates the hypertrophic cardiomyocyte growth induced by angiotensin II. J. Clin. Invest. 109, 787–796.
Sperr, W.R., et al., 1994. The human cardiac mast cell: localization, isolation, phenotype, and functional characterization. Blood 84, 3876–3884.
Steingrimsson, E., et al., 2004. Melanocytes and the microphthalmia transcription factor network. Annu. Rev. Genet. 38, 365–411.
Steingrimsson, E., et al., 1994. Molecular basis of mouse microphthalmia (mi) mutations helps explain their developmental and phenotypic consequences. Nat. Genet. 8, 256–263.
Tharp, M.D., et al., 1985. Conjugated avidin binds to mast cell granules. J. Histochem. Cytochem. 33, 27–32.

Tojo, H., Urata, H., 2013. Chymase inhibition and cardiovascular protection. Cardiovasc. Drugs Ther. 27, 139–143.
Tshori, S., et al., 2006. Transcription factor MITF regulates cardiac growth and hypertrophy. J. Clin. Invest. 116, 2673–2681.
Tshori, S., et al., 2007. Microphthalmia transcription factor isoforms in mast cells and the heart. Mol. Cell. Biol. 27, 3911–3919.
Urata, H., et al., 1993. Cellular localization and regional distribution of an angiotensin II-forming chymase in the heart. J. Clin. Invest. 91, 1269–1281.
Yajima, I., Larue, L., 2008. The location of heart melanocytes is specified and the level of pigmentation in the heart may correlate with coat color. Pigment Cell Melanoma Res. 21, 471–476.